V.O. KRASNOV

Institute for Condensed Matter Physics, Nat. Acad. of Sci. of Ukraine
(1, Svientsitskii Str., Lviv 79011, Ukraine; e-mail: krasnoff@icmp.lviv.ua)

PACS 67.85.Hj, 67.60.Fp, 71.10Fd

FERMION SPECTRUM OF BOSE–FERMI–HUBBARD MODEL IN THE PHASE WITH BOSE–EINSTEIN CONDENSATE

We investigate the fermion spectrum within the Bose–Fermi–Hubbard model used for the description of boson-fermion mixtures of ultra-cold atoms in optical lattices. We used the method based on the Hubbard operator approach for an on-site basis. The equation for fermion Green's function in the Bose–Fermi–Hubbard model is built; Green's functions of higher orders are decoupled in the Hubbard-I approximation (the case of the strong on-site interaction). The corresponding spectral densities are calculated. In the case of hard-core bosons, the condition of appearance of additional bands in the fermion spectrum is investigated. It is shown that these bands exist only in the state with a Bose–Einstein condensate and appear because of the mixing of states with different numbers of bosons. These additional bands can be interpreted as a manifestation of composite excitations (when the appearance of a fermion on the site is accompanied by the simultaneous creation (or annihilation) of a boson).

K e y w o r d s: Bose–Fermi–Hubbard model, optical lattices, Green's function, Bose–Einstein condensate, energy spectrum.

1. Introduction

The ultra-cold boson-fermion mixtures in optical lattices are the object of an intense theoretical investigation during last years both experimentally and theoretically. As in the case of a pure system of Bose-atoms, the transitions between the normal phase (phase of the so-called Mott insulator (MI)) with the integer occupation (at $T = 0$) of the local particle positions and the phase with a Bose–Einstein (BE) condensate (superfluid (SF) phase) take place in the mixtures. Among the important problems, one should mention, on the one hand, the influence of Fermi-atoms on the BE-condensation, and, on the other hand, the manifestation of the latter in the peculiarities and a reconstruction of the fermion energy spectrum.

The experimental verification of the superfluid–Mott insulator (SF–MI) transition in ultracold atomic gases was done by Greiner at al. [1]. There was supposed that the atomic gas in the Mott insulator phase can be considered as a new state of matter with unique properties.

Later, Ospelkaus *et al.* [2] observed a localized phase of ultracold bosonic quantum gases in a 3-dimensional optical lattice induced by a small contribution of fermionic atoms acting as impurities in a Fermi–Bose quantum gas mixture. They studied the dependence of this transition on the fermionic ^{40}K impurity concentration by a comparison to the corresponding superfluid–Mott insulator transition in a pure bosonic ^{87}Rb gas and found a significant shift in the transition parameters.

In theoretical investigations, the mixture of Bose–Fermi atoms in optical lattices was studied within the Bose–Fermi–Hubbard model (BFHM) [3–9]. According to the model, the key role in the MI-SF phase transitions belongs to the interplay between the tendency to a localization at the lattice sites and

the short-range interaction between particles, as well as the intersite particle hopping. The general Bose–Fermi–Hubbard Hamiltonian for a one-dimensional optical lattice with a superimposed harmonic trapping potential was derived in [3]. The conditions of stability of the mixture and a mean-field criterion for the onset of a bosonic superfluid transition were studied. In addition, the existence of a disordered phase for mixtures loaded in very deep lattices was predicted.

Buchler *et al.* showed [4] that a two-dimensional atomic mixture of bosons and fermions cooled into their quantum degenerate states and subjected to an optical lattice develops a supersolid phase characterized by the simultaneous presence of a nontrivial crystalline order and a phase order. This transition is in competition with the phase separation.

Lewenstein *et al.* discussed [5] the phase diagram at low temperatures and in the limit of strong atom-atom interactions. They predicted the existence of quantum phases that involve the pairing of fermions with one or more bosons or, alternatively, bosonic holes. These resulting composite fermions may form, depending on parameters of the system, a normal Fermi liquid, a density wave, a superfluid liquid, or an insulator with fermionic domains.

The Fermi–Bose version of the Falicov–Kimball model on a periodic lattice was considered to describe Fermi–Bose mixtures consisting of light fermions and heavy bosons that are loaded into optical lattices (ignoring the trapping potential) [6]. It was studied (within the dynamical mean-field theory (DMFT)) how the occupancy of bosons, single-particle many-body density of states for fermions, momentum distribution, and average kinetic energy evolve with the temperature. Within a similar approach, it was shown in [7] that a mixture of strongly interacting bosons and spinless fermions with on-site repulsion in a three-dimensional optical lattice is unstable against the phase separation for a weak repulsion among the bosons.

The case of hard-core bosons was considered, and the pseudospin formalism was used to describe the phase transitions at finite temperatures in the Bose–Fermi–Hubbard model in the self-consistent random phase approximation [8] and the mean-field approximation for a lattice with two nonequivalent sublattices [9]. It was shown in those works that the transitions between the uniform and charge-ordered phases

can be of the second or first order, depending on parameters of the system. It is possible also the existence of the supersolid phase.

The investigation of the fermion spectrum of BFHM and its transformation, when the Bose–Einstein condensate (the SF-phase) appears, is an interesting problem. Earlier [10], the thermodynamics of the model was investigated in the mean-field approximation (MFA); the influence of the fermion subsystem was studied, and phase diagrams illustrating the MI-SF phase transition were built. Here, we are going beyond the MFA and will calculate the fermion band spectrum, as well as single-particle density of states, by using the Green's function technique and considering the strong on-site interactions.

2. Hamiltonian of the Model and its Transformation

The mixtures of ultracold bosons and spin-polarized fermions in optical lattices are well described by the Bose–Fermi–Hubbard Hamiltonian [8–10] in terms of the operators of creation and annihilation of bosons (b^+, b) and fermions (a^+, a):

$$H = \sum_{<i,j>} t_{ij} b_i^+ b_j + \sum_{<i,j>} t'_{ij} a_i^+ a_j +$$

$$+ \frac{U}{2} \sum_i n_i^b (n_i^b - 1) + U' \sum_i n_i^b n_i^f -$$

$$- \mu \sum_i n_i^b - \mu \sum_i n_i^f. \tag{1}$$

The first (second) term describes the nearest neighbor boson (fermion) hopping between the nearest lattice sites (nearest potential minima in an optical lattice) with the $t(t')$ parameter denoting the tunneling amplitude of bosons (fermions). The third and fourth terms describe the on-site boson-boson and boson-fermion interactions, respectively. The last two terms involve the chemical potentials of bosons μ and fermions μ', which are introduced, when the grand canonical ensemble is used.

The type of a lattice is not get specified. In the numerical calculations (see below), we use the semielliptic density of states that corresponds approximately to a simple cubic lattice.

We use the approach of spinless fermions. In the mixtures with ultracold fermions in optical lattices, such a representation can be used in the situation where a strong magnetic field is applied. The fermion spins are oriented in one direction in this case.

Here, the single-site basis $|n_B, n_F\rangle$ is denoted as $|n\rangle = |n, 0\rangle, |\widetilde{n}\rangle = |n, 1\rangle$; $n_B(n_F)$ is the boson (fermion) occupation number.

After introducing the Hubbard operators $X_i^{mn} = |n, i\rangle\langle m, i|$, we have (see [10])

$$\hat{H} = \sum_{i,n} \lambda_n X_i^{nn} + \sum_{i,\widetilde{n}} \lambda_{\widetilde{n}} X_i^{\widetilde{n}\widetilde{n}} + \sum_{<i,j>} t'_{ij} a_i^+ a_j +$$

$$+ \sum_{<i,j>} t_{ij} b_i^+ b_j, \tag{2}$$

where

$$\lambda_n = \frac{U}{2} n(n-1) - n\mu,$$

$$\lambda_{\widetilde{n}} = \frac{U}{2} \widetilde{n}(\widetilde{n}-1) - \mu\widetilde{n} - \mu' + U'\widetilde{n} \tag{3}$$

and

$$b_i = \sum_n \sqrt{n+1} X_i^{n,(n+1)} + \sum_{\widetilde{n}} \sqrt{\widetilde{n}+1} X_i^{\widetilde{n},(n+1)},$$

$$a_i = \sum_n X_i^{n,\widetilde{n}}. \tag{4}$$

Here, $\lambda_{n(\widetilde{n})}$ are the energies of single-site states with n bosons and zero (one) fermion on a lattice site.

To investigate the fermion energy spectrum of the boson-fermion mixture described by Hamiltonian (2), the calculation of two-time temperature Green's function $\langle\langle a|a^+\rangle\rangle_{\omega,q}$ constructed on the annihilation and creation operators will be performed. Its poles will give a single-particle spectrum, while the imaginary part (after the analytical continuation $\omega \to \omega - i\varepsilon$) will determine a density of fermion states. In our case, this means that we have to find Green's function built on the Hubbard operators $\langle\langle X^{n\widetilde{n}}|X^{\widetilde{r}r}\rangle\rangle$. A similar representation was used before in [11], where the electron energy spectrum of the pseudospin-electron model was calculated within the framework of the dynamical mean-field theory (DMFT), and the alloy-analogy approximation. The effect of the pseudospin-electron interaction, local asymmetry field, and tunneling-like level splitting on the existence and the number of electron subbands was investigated.

Let us use the equation of motion

$$\hbar\omega\langle\langle A|B\rangle\rangle = \frac{\hbar}{2\pi}[A, B] + \langle\langle[A, H]|B\rangle\rangle. \tag{5}$$

We need now to find the following commutators:

$$\left[X_p^{m,\widetilde{m}}, \sum_{i,n} \lambda_n X_i^{nn} + \sum_{i,\widetilde{n}} \lambda_{\widetilde{n}} X_i^{\widetilde{n}\widetilde{n}}\right] =$$

$$= (\lambda_{\widetilde{m}} - \lambda_m) X_p^{m,\widetilde{m}} = (U'\widetilde{m} - \mu') X_p^{m,\widetilde{m}}, \tag{6}$$

$$\left[X_p^{m,\widetilde{m}}, \sum_{<i,j>} t_{ij} b_i^+ b_j + \sum_{<i,j>} t'_{ij} a_i^+ a_j\right] =$$

$$= \sum_j t_{pj} \left(-\sqrt{m+1} X_p^{m+1,\widetilde{m}} + \sqrt{\widetilde{m}} X_p^{m,\widetilde{m}-1}\right) b_j +$$

$$+ \sum_i t_{ip} b_i^+ \left(-\sqrt{m} X_p^{m-1,\widetilde{m}} + \sqrt{\widetilde{m}+1} X_p^{m,\widetilde{m}+1}\right) +$$

$$+ \sum_j t'_{pj} \left(X_p^{mm} + X_p^{\widetilde{m}\widetilde{m}}\right) a_j. \tag{7}$$

In what follows, we will use the decouplings (see [10]), which are equivalent to the mean-field approximation in the case of bosons and to the Hubbard-I approximation for fermions. Such an approximation, as is known from the theory of strongly correlated electron systems [12], goes beyond the mean-field approach separating the contributions from various configurations of the local state occupation (due to employing the Hubbard basis, the on-site interaction U' is taken in the zero approximation into account). In (7), we replace

$$b_j \to \langle b_j \rangle \equiv \varphi, \quad b_i^+ \to \langle b_j^+ \rangle \equiv \varphi^* = \varphi,$$

$$(X_p^{mm} + X_p^{\widetilde{m}\widetilde{m}}) \to \langle X^{mm} + X^{\widetilde{m}\widetilde{m}} \rangle, \tag{8}$$

taking into account that our system can be in the state with the uniform Bose–Einstein condensate (BEC) characterized by the order parameter φ.

Then

$$\left[X_p^{m,\widetilde{m}}, \sum_{<i,j>} t_{ij} b_i^+ b_j + \sum_{<i,j>} t'_{ij} a_i^+ a_j\right] =$$

$$= t_0 \varphi \left(-\sqrt{m+1} X_p^{m+1,\widetilde{m}} + \sqrt{\widetilde{m}} X_p^{m,\widetilde{m}-1}\right) +$$

$$+ t_0 \varphi_i^* \left(-\sqrt{m} X_p^{m-1,\widetilde{m}} + \sqrt{\widetilde{m}+1} X_p^{m,\widetilde{m}+1}\right) +$$

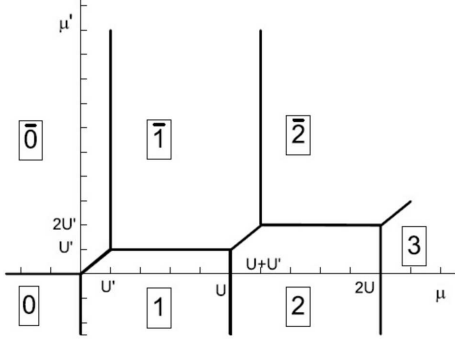$$+ \sum_j t'_{pj} \langle X^{mm} + X^{\widetilde{m}\widetilde{m}}\rangle a_j, \tag{9}$$

Fig. 1. Ground-state diagram for $0 < U' < U$. The regions which correspond to the unperturbed ground state $|m\rangle$ or $|\widetilde{m}\rangle$ are indicated by numbers

where $t_0 = \sum_{i,j} t_{ij} \equiv t_{\mathbf{q}=0}$. Due to the translational invariance, $t_{ij} = t(\mathbf{R}_i - \mathbf{R}_j)$; because of that, at the transition to the wave vector representation, the Fourier transform reads

$$t_{\mathbf{q}} = \sum_j e^{i\mathbf{q}(\mathbf{R}_i - \mathbf{R}_j)} t_{ij}. \qquad (10)$$

Finally, we get an equation for Green's function $\langle\langle X^{m\widetilde{m}} | X^{\widetilde{n}n}\rangle\rangle$. In the case of closely related levels $\lambda_m, \lambda_{\widetilde{m}}$ and $\lambda_{\widetilde{m}-1}$, this equation can be simplified and written in the form

$$\hbar\omega\langle\langle X_p^{m\widetilde{m}} | X_r^{\widetilde{n}n}\rangle\rangle = \frac{\hbar}{2\pi}\delta_{pr}\delta_{mn}\delta_{\widetilde{m}\widetilde{n}}\langle X^{mm} + X^{\widetilde{m}\widetilde{m}}\rangle +$$

$$+ (U'\widetilde{m} - \mu')\langle\langle X_p^{m\widetilde{m}} | X_r^{\widetilde{n}n}\rangle\rangle +$$

$$+ t_0\varphi\sqrt{\widetilde{m}}\langle\langle X_p^{m\widetilde{m}-1} | X_r^{\widetilde{n}n}\rangle\rangle +$$

$$+ \sum_j t'_{pj}\langle X^{mm} + X^{\widetilde{m}\widetilde{m}}\rangle\langle\langle a_j | X_r^{\widetilde{n}n}\rangle\rangle. \qquad (11)$$

One can see that, in order to obtain a closed system of equations, we need to find Green's function $\langle\langle X_p^{m\widetilde{m}-1} | X_r^{\widetilde{n}n}\rangle\rangle$. To calculate it, we use the similar steps and approximations done before for the function $\langle\langle X_p^{m\widetilde{m}} | X_r^{\widetilde{n}n}\rangle\rangle$. Finally, we have

$$\hbar\omega\langle\langle X_p^{m\widetilde{m}-1} | X_r^{\widetilde{n}n}\rangle\rangle =$$

$$= \frac{\hbar}{2\pi}\delta_{pr}\left(\delta_{mn}\langle X^{\widetilde{n}\widetilde{m}-1}\rangle + \delta_{\widetilde{m}-1,\widetilde{n}}\langle X^{mn}\rangle\right) +$$

$$+ (\lambda_{\widetilde{m}-1} - \lambda_m)\langle\langle X_p^{m\widetilde{m}-1} | X_r^{\widetilde{n}n}\rangle\rangle +$$

$$+ t_0\varphi^*\sqrt{\widetilde{m}}\langle\langle X_p^{m\widetilde{m}} | X_r^{\widetilde{n}n}\rangle\rangle + \sum_j t'_{pj}\frac{\varphi^*}{\sqrt{\widetilde{m}}}\langle\langle a_j | X_r^{\widetilde{n}n}\rangle\rangle.$$

$$(12)$$

By passing, similarly to (10), to the Fourier transforms of hopping parameters and Green's functions, we obtain the final system of equations

$$(\hbar\omega - U'm + \mu') G^{m\widetilde{m},\widetilde{n}n}(\omega, q) =$$

$$= \frac{\hbar}{2\pi}\delta_{mn}\delta_{\widetilde{m}\widetilde{n}}\langle X^{mm} + X^{\widetilde{m}\widetilde{m}}\rangle +$$

$$+ t_0\varphi\sqrt{\widetilde{m}}G^{m\widetilde{m}-1,\widetilde{n}n}(\omega, q) +$$

$$+ t'_q\langle X^{mm} + X^{\widetilde{m}\widetilde{m}}\rangle\langle\langle a | X^{\widetilde{n}n}\rangle\rangle_{\omega,q}, \qquad (13)$$

$$(\hbar\omega - \lambda_{\widetilde{m}-1} + \lambda_m) G^{m\widetilde{m}-1,\widetilde{n}n}(\omega, q) =$$

$$= \frac{\hbar}{2\pi}\left(\delta_{mn}\langle X^{\widetilde{n}\widetilde{m}-1}\rangle + \delta_{\widetilde{m}-1,\widetilde{n}}\langle X^{mn}\rangle\right) +$$

$$+ t_0\varphi\sqrt{\widetilde{m}}G^{m\widetilde{m},\widetilde{n}n}(\omega, q) +$$

$$+ \frac{t'_q\varphi^*}{\sqrt{\widetilde{m}}}\langle\langle a | X^{\widetilde{n}n}\rangle\rangle_{\omega,q}. \qquad (14)$$

3. Four-State Approximation

Let us simplify the set of equations (13) and (14), by using an approach where a finite number of single-site states $|n_{\mathrm{B}}, n_{\mathrm{F}}\rangle$ is taken into account. In our earlier paper [10], we investigated the ground-state diagrams for the Bose–Fermi–Hubbard model without hopping.

In Fig. 1, we show one of them, by assuming $0 < U' < U$.

Supposing that $U \to \infty$ (the hard-core boson limit), we restrict ourselves to the case where only four states can be considered:

$|0\rangle$ – no bosons or fermions on the site,

$|\widetilde{0}\rangle$ – no bosons, but one fermion on the site,

$|1\rangle$ – one boson and no fermions on the site,

$|\widetilde{1}\rangle$ – one boson and one fermion on the site.

This approximation is also valid, when U (energy of the boson on-site repulsion) is much greater than U' (on-site fermion interaction), see Fig. 1.

A situation where the on-site repulsion of bosons U is considerable is realized in optical lattices in the case of deep potential wells (what is reached by a growth of the intensity of laser beams). On the other hand, the U' parameter can be changed within a wide enough range adjusting the experimental conditions [15].

Then we will have four energy levels

$$\lambda_0 = 0, \lambda_{\widetilde{0}} = -\mu', \lambda_1 = -\mu, \lambda_{\widetilde{1}} = -\mu - \mu' + U' \quad (15)$$

and, for Bose- and Fermi-operators,

$$a_i = X_i^{0,\widetilde{0}} + X_i^{1,\widetilde{1}}, \quad b_i = X_i^{0,1} + X_i^{\widetilde{0},\widetilde{1}}. \qquad (16)$$

The decouplings $b_i \to \varphi, b_i^+ \to \varphi$ in the equations of motion for Green's functions are equivalent to the choice of the single-site part of the full Hamiltonian in the mean-field form $H_i = \sum_{pr} H_{pr} X_i^{pr}$, where

$$||H_{pr}|| = \begin{pmatrix} & |0\rangle & |1\rangle & |\widetilde{0}\rangle & |\widetilde{1}\rangle & \\ \hline 0 & t_0\varphi & 0 & 0 & |0\rangle \\ t_0\varphi & -\mu & 0 & 0 & |1\rangle \\ 0 & 0 & -\mu' & t_0\varphi & |\widetilde{0}\rangle \\ 0 & 0 & t_0\varphi & -\mu - \mu' + U' & |\widetilde{1}\rangle \end{pmatrix}. \qquad (17)$$

Our next step is the diagonalization of matrix (17). For this purpose, we use the transformation

$$\hat{U}^T * \hat{H} * \hat{U} = \hat{\widetilde{H}}, \qquad (18)$$

where $\hat{U} = \begin{pmatrix} \hat{U}_1 & \hat{0} \\ \hat{0} & \hat{U}_2 \end{pmatrix}$,

$\hat{U}_1 = \begin{pmatrix} \cos\psi & -\sin\psi \\ \sin\psi & \cos\psi \end{pmatrix}$, and $\hat{U}_2 = \begin{pmatrix} \cos\widetilde{\psi} & -\sin\widetilde{\psi} \\ \sin\widetilde{\psi} & \cos\widetilde{\psi} \end{pmatrix}$.

Here,

$$\begin{aligned} \sin 2\psi &= \frac{t_0\varphi}{\sqrt{\mu^2/4 + t_0^2\varphi^2}}, \\ \sin 2\widetilde{\psi} &= \frac{t_0\varphi}{\sqrt{(U'-\mu)^2/4 + t_0^2\varphi^2}}. \end{aligned} \qquad (19)$$

Then we will get the diagonal single-site part (which is as well a mean-field one) of the Hamiltonian,

$$\hat{H}_0 = \sum_{p'} \varepsilon_{p'} X^{p'p'}, \qquad (20)$$

where $p' = 0', 1', \widetilde{0}', \widetilde{1}'$ are indices denoting the states of the new basis,

$$\begin{aligned} \varepsilon_{0',1'} &= -\frac{\mu}{2} \pm \sqrt{\frac{\mu^2}{4} + t_0^2\varphi^2}, \\ \varepsilon_{\widetilde{0}',\widetilde{1}'} &= -\mu' - \frac{\mu}{2} + \frac{U'}{2} \pm \sqrt{\frac{(U'-\mu)^2}{4} + t_0^2\varphi^2}. \end{aligned} \qquad (21)$$

In the new basis, the Fermi- and Bose-operators take the form

$$a_i = \cos\left(\widetilde{\psi} - \psi\right)\left(X_i^{0'\widetilde{0}'} + X_i^{1'\widetilde{1}'}\right) +$$

$$+ \sin\left(\widetilde{\psi} - \psi\right)\left(X_i^{1'\widetilde{0}'} - X_i^{0'\widetilde{1}'}\right),$$

$$\begin{aligned} b_i &= \frac{1}{2}\sin(2\psi)\left(X_i^{0'0'} - X_i^{1'1'}\right) + \\ &+ \frac{1}{2}\sin(2\widetilde{\psi})\left(X_i^{\widetilde{0}'\widetilde{0}'} - X_i^{\widetilde{1}'\widetilde{1}'}\right) + \\ &+ \cos^2\psi X_i^{0'1'} - \sin^2\psi X_i^{1'0'} + \\ &+ \cos^2\widetilde{\psi} X_i^{\widetilde{0}'\widetilde{1}'} - \sin^2\widetilde{\psi} X_i^{\widetilde{1}'\widetilde{0}'}. \end{aligned} \qquad (22)$$

Writing down the equations similar to (13) and (14), we can easily get the following expression for Green's function built on Fermi operators:

$$\langle\langle a|a^+\rangle\rangle = \frac{1}{2\pi}\frac{1}{g_0^{-1}(\omega) - t_q'}. \qquad (23)$$

Here,

$$\begin{aligned} g_0(\omega) &= \\ &= \cos^2(\widetilde{\psi}-\psi)\left[\frac{\langle X^{0'0'} + X^{\widetilde{0}'\widetilde{0}'}\rangle}{\hbar\omega - \varepsilon_{\widetilde{0}'} + \varepsilon_{0'}} + \frac{\langle X^{1'1'} + X^{\widetilde{1}'\widetilde{1}'}\rangle}{\hbar\omega - \varepsilon_{\widetilde{1}'} + \varepsilon_{1'}}\right] + \\ &+ \sin^2(\widetilde{\psi}-\psi)\left[\frac{\langle X^{1'1'} + X^{\widetilde{0}'\widetilde{0}'}\rangle}{\hbar\omega - \varepsilon_{\widetilde{0}'} + \varepsilon_{1'}} + \frac{\langle X^{0'0'} + X^{\widetilde{1}'\widetilde{1}'}\rangle}{\hbar\omega - \varepsilon_{\widetilde{1}'} + \varepsilon_{0'}}\right] \end{aligned} \qquad (24)$$

is the single-site Green's function.

4. Fermion Spectrum at $T = 0$

Now, we will analyze the ground state of our system in the presence of BEC. This means that we need to analyze the behavior of single-site energy levels of the system given by formulae (21). In the case $T = 0$, only the states with the lowest energy values will contribute to expression (24) for $g_0(\omega)$.

In this connection, we have to consider an equation for the order parameter with regard for the possibility of different ground states. In the ground state $|\widetilde{1}'\rangle$ (when $\langle X^{\widetilde{1}'\widetilde{1}'}\rangle = 1$, and the other averages are equal to zero), the order parameter $\varphi \equiv \langle b\rangle$ from (22) satisfies the equation

$$\varphi = -\frac{1}{2}\sin(2\widetilde{\psi}) = \frac{|t_0|\varphi}{\sqrt{\frac{(U'-\mu)^2}{4} + t_0^2\varphi^2}}. \qquad (25)$$

The solution $\varphi = 0$ corresponds to the normal (Mott insulator) phase; $\varphi \neq 0$ describes the phase with BEC. For this phase, Eq. (25) yields

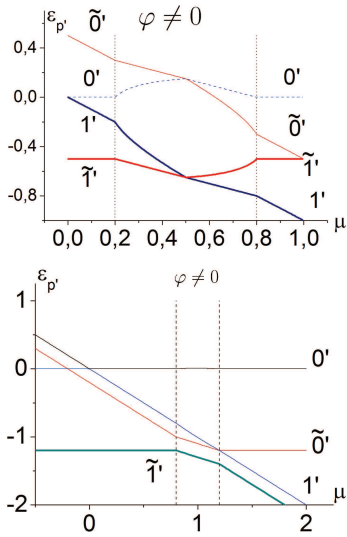$$\varphi = \frac{1}{2}\sqrt{1 - \frac{(U'-\mu)^2}{t_0^2}}. \qquad (26)$$

Fig. 2. On-site energies $\varepsilon_{p'}$ for $\mu' = 0.5$, $t_0 = -0.8$ (upper graph) and $\mu' = 1.2$, $t_0 = -0.2$ (lower graph)
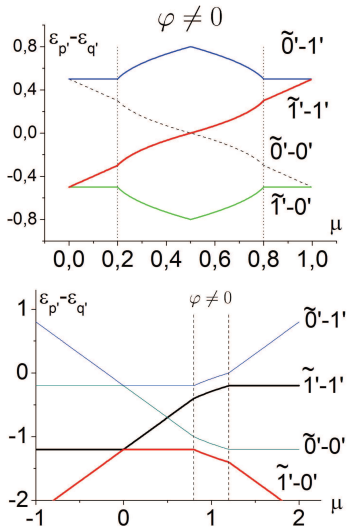

Fig. 3. Energy transitions $\varepsilon_{p'} - \varepsilon_{q'}$ for $\mu' = 0.5, t_0 = -0.8$ (upper graph) and $\mu' = 1.2, t_0 = -0.2$ (lower graph)

In the same way, when the ground state is $|1'\rangle$, we have

$$\varphi = \frac{1}{2}\sqrt{1 - \frac{\mu^2}{t_0^2}}. \tag{27}$$

When the boson chemical potential μ is changed (see Fig. 2), two cases are possible: with or without a change of the ground state. On the first graph, the situation is shown, when we have the ground states

$|\widetilde{1}'\rangle$ at $\mu < \mu'$ and $|1'\rangle$ at $\mu > \mu'$. On the second graph, the case is presented, when only the ground state $|\widetilde{1}'\rangle$ is realized (here, the states $|\widetilde{1}'\rangle$ and $|1'\rangle$ belong to the transformed basis).

Let $T = 0$. If the ground state is $|\widetilde{1}'\rangle$, then we have only $\langle X^{\widetilde{1}'\widetilde{1}'}\rangle = 1$. For other states, we have $\langle X^{p'p'}\rangle = = 0$. This means that, in this case, Eq. (24) yields

$$g_0(\omega) = \cos^2(\widetilde{\psi} - \psi)\frac{\langle X^{1'1'} + X^{\widetilde{1}'\widetilde{1}'}\rangle}{\hbar\omega - \varepsilon_{\widetilde{1}'} + \varepsilon_{1'}} +$$

$$+ \sin^2(\widetilde{\psi} - \psi)\frac{\langle X^{0'0'} + X^{\widetilde{1}'\widetilde{1}'}\rangle}{\hbar\omega - \varepsilon_{\widetilde{1}'} + \varepsilon_{0'}} \equiv$$

$$\equiv \frac{\cos^2(\widetilde{\psi} - \psi)}{\hbar\omega - \varepsilon_{\widetilde{1}'} + \varepsilon_{1'}} + \frac{\sin^2(\widetilde{\psi} - \psi)}{\hbar\omega - \varepsilon_{\widetilde{1}'} + \varepsilon_{0'}}. \tag{28}$$

Here, only the energy transitions involving the ground state $|\widetilde{1}'\rangle$ contribute (see Fig. 3).

Then we obtain the following expression for fermion Green's function:

$$\langle\langle a|a^+\rangle\rangle = \frac{1}{2\pi}\frac{1}{g_0^{-1}(\omega) - t_k} =$$

$$= \frac{1}{2\pi}\frac{(\hbar\omega - \Delta_{\widetilde{1}'0'})\cos^2(\widetilde{\psi} - \psi) + (\hbar\omega - \Delta_{\widetilde{1}'1'})\sin^2(\widetilde{\psi} - \psi)}{\det}. \tag{29}$$

Here,

$$\det = (\hbar\omega - \Delta_{\widetilde{1}'0'})(\hbar\omega - \Delta_{\widetilde{1}'1'}) +$$

$$+ t_q(\hbar\omega - \Delta_{\widetilde{1}'0'})\cos^2(\widetilde{\psi} - \psi) +$$

$$+ t_q(\hbar\omega - \Delta_{\widetilde{1}'1'})\sin^2(\widetilde{\psi} - \psi), \tag{30}$$

and $\Delta_{m'n'} = \varepsilon_{m'} - \varepsilon_{n'}$.

This expression can be rewritten as the decomposition into simple fractions:

$$\langle\langle a|a^+\rangle\rangle = \frac{1}{2\pi}\left[\frac{A_1}{\hbar\omega - X_1} + \frac{A_2}{\hbar\omega - X_2}\right]. \tag{31}$$

Here, X_1 an X_2 are solutions of the quadratic (in the variable $\hbar\omega$) equation that determines the poles of function (30) (functions $\varepsilon_{1,2}(q) = X_{1,2}$ describe the dispersion laws for the fermion band spectrum), and A_1 and A_2 are constants in the fraction decomposition.

Finally, the density of fermion states is as follows:

$$\rho(\hbar\omega) = \frac{1}{\hbar N}\sum_q -2\operatorname{Im}(G_q(\omega + i\epsilon))_{\epsilon\to 0} =$$

$$= \int\limits_{-W}^{W} dx \rho_0(x)\Big(A_1(x)\delta(x - X_1) +$$

$$+ A_2(x)\delta(x - X_2)\Big). \tag{32}$$

Here, $\rho_0(x) = \frac{1}{N}\sum_q \delta(x - t_q)$ is the unperturbed density of states (DOS).

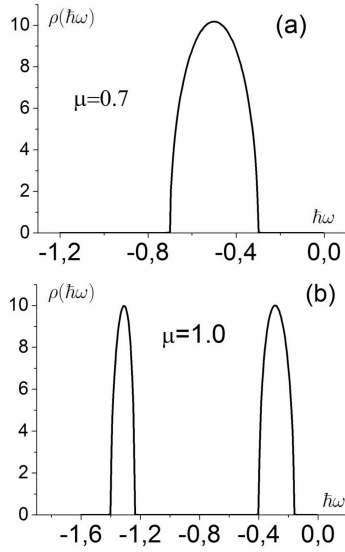The expressions similar to (29),(31), and (32) can be obtained in the case with the ground state $|1'\rangle$.

5. Results

We illustrate the results of numerical calculations, by using the following values of the model parameters. The constant of the boson-fermion on-site interaction U' is taken as the energy unit $U' = 1$. Other energy quantities are given in relation to U': the boson hopping constant is $t_0 = -0.2$ and -0.8; the half-width of the unperturbed fermion band described by the semielliptic DOS $\rho_0(\omega) = \frac{1}{2W}\sqrt{W^2 - \omega^2}$ is
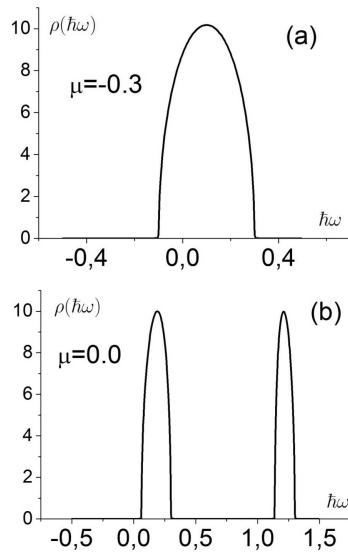

Fig. 4. Density of fermion states for various μ, when $\mu' = 1.2$, $t_0 = -0.2$

Fig. 6. Density of fermion states for various μ, when $\mu' = -0.1$, $t_0 = -0.2$

Fig. 5. Fermion energy bands (upper graph) and the order parameter (lower graph) for $\mu' = 1.2$, $t_0 = -0.2$
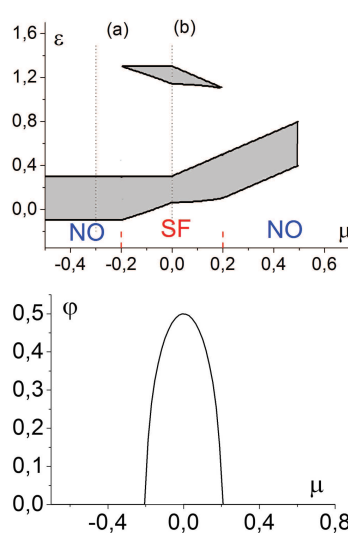

Fig. 7. Fermion energy bands (upper graph) and the order parameter (lower graph) for $\mu' = -0.1$, $t_0 = -0.2$
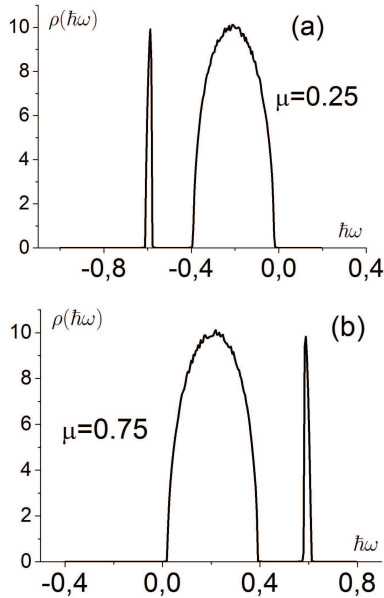
Fig. 8. Density of fermion states for various μ, when $\mu' = 0.5$, $t_0 = -0.8$
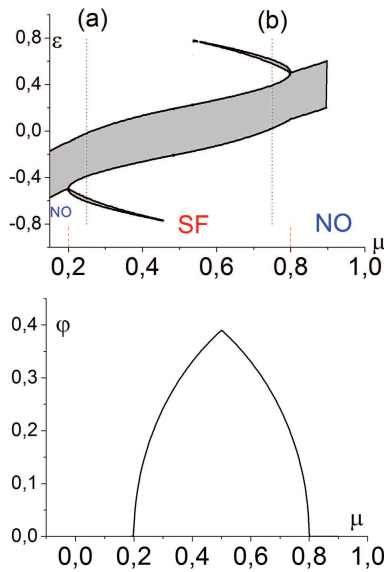

Fig. 9. Fermion energy bands (upper graph) and the order parameter (lower graph) for $\mu' = 0.5$, $t_0 = -0.8$

$W \equiv t'_0 = 0.2$ (a case of narrow band). It should be mentioned that a change of the model parameters values does not influence significantly the structure of the fermion spectrum. In real systems, they depend on the conditions of experiments and can be varied [16].

Accordingly to the ground state diagram (see Fig. 1), we studied three cases with different values of fermion chemical potential:

$\mu' = -0.1$ (the $|0\rangle \rightarrow |1\rangle$ transition (at the change of μ) in terms of unperturbed single-site states);

$\mu' = 0.5$ (the transition with the change of the ground state from $|\tilde{1}\rangle$ to $|1\rangle$, *ibid.*);

$\mu' = 1.2$ (the $|\tilde{0}\rangle \rightarrow |\tilde{1}\rangle$ transition *ibid.*).

The results of calculations of the density of states $\rho(\hbar\omega)$ according to (32) for various values of bosonic chemical potential μ are presented in Figs. 4, 6, and 8.

The fermion energy bands (as regions, where $\rho(\hbar\omega) \neq 0$) and the order parameter φ as functions of μ are given in Figs. 5, 7, and 9.

From these results, one can see that, in addition to a shift of the fermion bands that depends on the chemical potential of bosons (and, consequently, on the boson concentration), the appearance of new fermion subbands additionally to the traditional Hubbard-like ones in the SF phase (the phase with BE-condensate, where $\varphi \neq 0$) takes place. We think that this is due to the mixing of states with different numbers of bosons and the possibility of new fermion transitions, which are accompanied by the creation or annihilation of bosons. Such excitations are called "composite fermions" and were earlier described in [13, 14].

6. Conclusions

In a pure boson system described by the Bose–Hubbard model, the SF phase exists at $T = 0$ on the intervals of μ values, which have the widths proportional to t_0 and are centered at the points $\mu = nU$. In the hard-core boson limit ($U \rightarrow \infty$), only one such region remains with the center at the $\mu = 0$ point. It separates two regions that correspond to the normal (MI) phases with $\langle n_B \rangle = 0$ and $\langle n_B \rangle = 1$, respectively. In the presence of fermions, the region of existence of the SF phase in the case $\mu' < 0$ remains the same. However, when $\mu' > U'$, such a region is centered at the $\mu = U'$ point. Here, the BE-condensation takes place in the lattice with $\langle n_F \rangle = 1$, while $\langle n_F \rangle = 0$ in the previous case. The more complicated situation is observed in the intermediate range of the μ' values. The borders of the SF region shift with a change of the relation between t_0 and U' parameters.

The unperturbed fermion band is a single band; its width is proportional to the hopping parameter t'. The interaction between Bose- and Fermi-particles described by BFHM leads to changes in the spectrum of fermions. At $T = 0$, two factors influence the form of the spectrum: (i) a change of the ground state, which is possible for $0 < \mu' < U'$ and takes place at the certain value of chemical potential μ of bosons; (ii) the presence of the BE-condensate (in the SF phase).

In the normal (NO) phase, a change of the ground state leads to a shift of the fermion band. The reason for this effect is the following. The transitions that form the band happen actually between the states $|n, 0\rangle$ and $|n, 1\rangle$ with the same number of bosons; the latter can be different. The band shift (at $n = 1$ regarding to the $n = 0$ case) is of the order of the interaction constant U' (the appearance of a fermion on the site, where a boson is already present, causes the energy increase by U').

Let us the case of the SF phase with a BE-condensate. In addition to the above-mentioned shift of the fermion bands that depends on boson chemical potential (boson concentration, as a result), the splitting of the spectrum and the appearance of new fermion subbands in the SF-phase (the phase with BE-condensate) take place. The effect occurs in the region of boson chemical potential μ values, where the order parameter φ differs from zero. Its physical background consists in the mixing of states with different numbers of bosons and the possibility of new fermion transitions, which are accompanied by the creation or annihilation of bosons. Such excitations are called "composite fermions" [13, 14]. We see their manifestation in the fermion spectrum. The presented results are restricted to the $T = 0$ limit. At finite temperatures, the new subbands will appear (four subbands in the case of the 4-state model). A similar effect of the fermion spectrum splitting was obtained previously for the pseudospin-electron model [11], where the calculations were performed within the DMFT approach. The more complete analysis of a reconstruction of the energy spectrum in the case $T \neq 0$, especially in the intermediate region $0 < \mu' < U'$, will be a subject of our subsequent consideration.

1. M. Greiner *et al.*, Nature, **415**, 39 (2002).
2. S. Ospelkaus, C. Ospelkaus, O. Wille *et al.*, Phys. Rev. Lett. **96**, 180403 (2006).
3. A. Albus, F. Illuminati, and J. Eisert, Phys. Rev. A **68**, 023606 (2003).
4. H.P. Buchler and G. Blatter, Phys. Rev. Lett. **91**, 130404 (2003).
5. M. Lewenstein, L. Santos, M.A. Baranov, and H. Fehrmann, Phys. Rev. Lett. **92**, 050401 (2004).
6. M. Iskin and J.K. Freericks, Phys. Rev. A **80**, 053623 (2009).
7. I. Titvinidze, M. Snoek, and W. Hofstetter, Phys. Rev. Lett. **100**, 100401 (2008).
8. T.S. Mysakovych, J. Phys.: Condens. Matter **22**, 355601 (2010).
9. T.S. Mysakovych, Condens. Matter Phys. **14**, No. 4, 43301 (2011).
10. I.V. Stasyuk, T.S. Mysakovych, and V.O. Krasnov, Condens. Matter Phys. **13**, No. 1, 13003 (2010).
11. I.V. Stasyuk and V.O. Krasnov, Ukr. J. Phys. **58**, 68 (2013).
12. J. Hubbard, Proc. Roy. Soc. Lond. A. **276**, 238 (1963).
13. H. Fehrmann, M. Baranov, M. Lewenstein, and L. Santos, Opt. Express **12**, 55 (2004).
14. R.M. Lutchyn, S. Tewari, and S. Das Sarma, Phys. Rev. B **78**, 220504(R) (2008).
15. S. Akhanjee, Phys. Rev. B **82**, 075138 (2010).
16. I. Bloch, J. Dalibard, and W. Zwerger, Rev. Mod. Phys. **80**, 885 (2008).

В.О. Краснов

ФЕРМІОННИЙ СПЕКТР
МОДЕЛІ БОЗЕ–ФЕРМІ–ХАББАРДА
У ФАЗІ З БОЗЕ-КОНДЕНСАТОМ

Р е з ю м е

Досліджено ферміонний спектр моделі Бозе–Фермі–Хаббарда. Ця модель використовується для опису бозон-ферміонних сумішей ультрахолодних атомів в оптичних ґратках. Застосовано підхід операторів Хаббарда на одновузловому базисі. Побудовано рівняння для ферміонних функцій Ґріна; розчеплення функцій Ґріна вищих порядків проведено в дусі наближення Хаббард-I (випадок сильної одновузлової взаємодії). Розраховано відповідні спектральні густини. Для випадку жорстких бозонів досліджено умови появи додаткових зон в ферміонному спектрі. Показано, що ці зони існують тільки за наявності бозе-конденсату та з'являються внаслідок переміщування станів з різним числом бозонів. Існування таких зон можна інтерпретувати як прояв композитних збуджень (коли поява ферміона на вузлі ґратки супроводжується одночасною появою (або зникненням) бозона).